Scientific paper

Electrochemical Detection of Nitrite in Food Based on Poly (3,4-ethylenedioxythiophene) Doped with Fe_3O_4 Nanoparticles Loaded Carboxylated Nanocrystalline Cellulose

Guiyun Xu, Mingming Zhang and Xijuan Yu*

Key Laboratory of Sensor Analysis of Tumor Marker, Ministry of Education, College of Chemistry and Molecular Engineering, Qingdao University of Science and Technology, Qingdao 266042, China

** Corresponding author: E-mail: xjuanyu@qust.edu.cn Tel:+ 86 532 84022681; Fax: + 86 532 84023927*

Received: 08-11-2017

Abstract

Carboxylated nanocrystalline cellulose (CNCC) was prepared by oxidation degradation of microcrystalline cellulose (MCC) using ammonium peroxydisulfate and modified with Fe_3O_4 nanoparticles to form Fe_3O_4-CNCC nanocomposite via simple refluxing process. The Fe_3O_4-CNCC nanocomposite doped poly(3,4-ethylenedioxythiophene) (PEDOT) was successfully decorated on the glassy carbon electrode (GCE) by electrochemical deposition. The PEDOT/Fe_3O_4-CNCC modified GCE with enlarged real electrochemical surface area was used to determine nitrite with high selectivity, sensitivity and outstanding reproducibility. Using amperometric current-time (i-t) curve, the proposed sensor provided a wider linear range (0.5–2500 μM) and a lower detection limit (0.1 μM) towards nitrite compared with the method of differential pulse voltammetry (DPV). This analytical method gave good selectivity in the practical measurement of nitrite in pickles.

Keywords: Carboxylated nanocrystalline cellulose; Fe_3O_4 nanoparticle; Poly(3, 4-ethylenedioxythiophene); Amperometric sensor; Nitrite

1. Introduction

Nanocellulose (NCC), one kind of sustainable functional nanomaterials, is derived from native cellulose.[1-5] Their morphology mainly depends on the source of precursor cellulose and the conditions of preparation. NCC exhibits remarkable properties, such as high surface area, thermally stable, renewable, biodegradable, non-toxic[6–8] and accessible industrially in large scale.[9] NCC has been extensively researched as key components in the design of super capacitors,[10–12] aerogels,[13] sensors,[14] pharmaceuticals,[15] chiral materials[16] and catalysts.[17] They are generated by the removal of amorphous regions of different sources of cellulose using acid hydrolysis, enzymatic or mechanical treatments. As a functional derivative of NCC, carboxylated nanocrystalline cellulose (CNCC) possesses better dispersibility and stability compared to NCC because of high density of carboxyl groups on its surface. In this work, CNCC was prepared using a strong oxidant, ammonium peroxydisulfate, instead of conventional acid hydrolysis.[18]

As an important magnetic nanomaterial, Fe_3O_4 magnetic nanoparticle received much attention and extensive investigation in the past years for its excellent electrocatalytic activity, biocompatibility and absorption ability.[19–23] For example, a sensitive electrochemical biosensor for the detection of H_2O_2 from living cells has been developed based on graphene blended with Fe_3O_4 nanoparticles.[24] Fe_3O_4 nanosphere decorated with Au nanoparticles was used as a kind of catalyst for the detection of As(III) in water.[25] However, Fe_3O_4 nanoparticles are thermodynamically unstable and tend to aggregate to form bulk particle. To overcome this problem, Fe_3O_4–CNCC was synthesized by dispersing Fe_3O_4 nanoparticles on the surface of CNCC in this work. Fe_3O_4-CNCC can be doped into poly(3,4-ethylenedioxythiophene) (PEDOT) to enhance its electrical conductivity.[26] Electrochemically polymerized PEDOT composites with different dopant have been widely used in various kinds of electrochemical sensors.[27–30]

Nitrite, a kind of food additive, is widely used in the food industry. However, excessive nitrite is detrimental to human health.[31,32] In human body, nitrite can lead to the irreversible oxidation reaction of hemoglobin to methemoglobin and also can be converted into nitrosamine, which would cause hypertension and cancer.[33] Therefore, the accurate detection of nitrite becomes a pressing issue both in the human body and food industries. Till now, various analytical techniques have been used to detect nitrite. For example, Zhang used chemiluminescence to detect nitrite with the detection limit of 0.024 μM.[34] Huang adopted spectrofluorimetry to determine nitrite in human saliva with the detection limit of 0.5 μM.[35] However, most of these methods are lengthy, expensive, require complicated procedure and expert knowledge that make them unsuitable for routine analysis. To the contrary, electrochemical techniques[36,37] provided a highly sensitive and rapid nitrite determination. Besides, the electrochemical approach was an environmentally friendly method because no extra chemical loading is required.

In this paper, Fe_3O_4-CNCC was synthesized through a simple refluxing process and then doped PEDOT onto a glass carbon electrode by electrochemical deposition. Combining the advantages of CNCC, Fe_3O_4, and PEDOT, the fabricated sensor can determine nitrite with high selectivity, sensitivity and outstanding reproducibility. This method gave good selectivity in the practical measurement of nitrite in pickles.

2. Experimental

2. 1. Materials

Microcrystalline cellulose with the length of 20–30 μm, ammonium peroxydisulfate (APS), 3,4-ethylenedioxythiophene (EDOT), ferrous sulfate ($FeSO_4$ $7H_2O$), ferric chloride ($FeCl_3$ $6H_2O$), ammonia solution (NH_3 H_2O), sodium nitrite ($NaNO_2$) were obtained from Aladin Ltd. (Shanghai, China). All chemicals used in this research were analytical grade. The 0.2 M phosphate buffer solutions (PBS, pH 7,4, containing 0.9% NaCl) was prepared by mixing stock solutions of 0.2 M NaH_2PO_4 and 0.2 M Na_2HPO_4 and it was used as supporting electrolyte in the detection of nitrite. Deionized water from a Milli-Q water purifying system was used throughout.

2. 2. Apparatus and Measurements

All electrochemical experiments were performed using a conventional three-electrode system containing a bare or PEDOT/CNCC, PEDOT/Fe_3O_4-CNCC modified glassy carbon working electrode (3 mm diameter), a platinum wire counter electrode and a saturated calomel reference electrode on a CHI660D (Shanghai CH Instruments Co., China) electrochemical work station. The structure and morphology of the samples were characterized by transmission electron microscopy (TEM; Hitachi High-Technology Co., Ltd., Japan) and field emission scanning electron microscopy (SEM; Hitachi High-Technology Co., Ltd., Japan). XRD spectra were recorded on an X-ray diffractometer (Shimadzu7000S, Shimadzu Analytical, Japan) equipped with CuKα radiation (λ = 0.154 nm). Zeta potentials of samples were measured with the Malvern Zetasizer Nano ZS90 (Malvern InstrumentsLtd., UK).

2. 3. Synthesis of CNCC

CNCC was prepared by a one-pot green procedure treatment of the mixture of MCC and APS. In brief, 2.5 g MCC and 57.05 g APS were dissolved in 250 mL of deionized water to form white suspension. The mixture was heated at 70 °C under stirring for 12 h to give a suspension of CNCC and then cooled to room temperature naturally. The suspension was centrifuged and washed with deionized water for several times until the pH of the suspension was close to that of deionized water. Finally, the product was lyophilized to yield a white powder.

2. 4. Synthesis of Fe_3O_4-CNCC Composite

Fe_3O_4-CNCC was synthesized through a simple refluxing process. Typically, 100 mL of the as-synthesized CNCC (8 mg mL^{-1}), 0.1127 g of $FeSO_4$ $7H_2O$ and 0.1918 g $FeCl_3$ $6H_2O$ were added to the three-necked flask. Then the pH value of solution was buffered close to 10 using 25 % NH_3 H_2O, and the solution was heated at 60 °C in flow of N_2 for 2 h. The prepared reaction products were put into the reaction still and heated at 80 °C for 2 h. The obtained solution was isolated in a centrifugal machine at the rate of 10000 rpm for 5 min and then washed thoroughly and dispersed with deionized water. Eventually, the Fe_3O_4-CNCC was composed following the processes discussed previously.

2. 5. Preparation of the PEDOT/Fe_3O_4-CNCC Modified Electrode

Before the modification, GCE was polished with 0.3 μm, 0.05 μm alumina slurries in sequence and then cleaned by ultrasonication in deionized water, ethanol and deionized water for 3 min, respectively. For preparation of PEDOT/Fe_3O_4-CNCC modified electrodes, CNCC-Fe_3O_4 nanocomposites were first decorated on the GCE by electrochemical deposition in a solution containing 1 mg mL^{-1} CNCC-Fe_3O_4 and 0.02 M EDOT. The electrodeposition was performed at a potential of 1.2 V (vs. SCE) for 180 s.

As control, PEDOT/CNCC modified electrode was prepared under the same conditions without the presence of Fe_3O_4. GCEs modified with the PEDOT/Fe_3O_4-CNCC and PEDOT/CNCC were denoted as PEDOT/Fe_3O_4–CNCC/GCE and PEDOT/CNCC/GCE, respectively.

2. 6. Electrochemical Measurements

Electrochemical impedance spectroscopy (EIS) measurements were recorded in 5.0 mM $[Fe(CN)_6]^{3-/4-}$ solution containing 0.1 M KCl within a frequency range of 1–100,000 Hz. The amplitude of the applied sine wave was 5 mV, and the direct current potential was set at 0.80 V. Both cyclic voltammetry (CV) and differential pulse voltammetry (DPV) used to study the electrochemical reaction of nitrite were carried out in 0.2 M phosphate buffered saline (PBS, pH 7.4, containing 0.9% NaCl) containing 5 mM nitrite. The CV was recorded from 0.4–1.1 V at a scan rate of 100 mV s^{-1}, while the DPV was performed from 0.4–1.4 V with the following parameters: pulse amplitude 50 mV; pulse width 0.2 s and pulse period 0.5 s. Amperometric current-time (i-t) curve was performed in stirring PBS (0.2 M, pH 7.4) with the potential set at 0.80 V. All experiments were conducted at ambient temperature.

2. 7. HPLC Measurements

The HPLC technique was employed as a reference method to measure nitrite in real samples. The measurement was based on the national standards of China (GB 5009.33–2016 [38]).

3. Results and Discussion

3. 1. Working Mechanism of PEDOT/Fe_3O_4-CNCC Modified Electrode

The electrode modification and electrocatalytic mechanism are shown in Fig 1. CNCC was prepared by degradation of MCC using ammonium peroxydisulfate, and then Fe_3O_4-CNCC was synthesized by a simple refluxing process. The obtained Fe_3O_4-CNCC nanocomposite doped poly(3,4-ethylenedioxythiophene) (PEDOT) was successfully decorated on the GCE by electrochemical deposition. The PEDOT/Fe_3O_4-CNCC modified electrode was used to determine nitrite in PBS. Based on the following results of the electrochemical tests, the corresponding transformation is shown as follows:

$$NO_2^- + H_2O - 2e^- \rightarrow NO_3^- + 2H^+.$$

3. 2. Characterization of the Fe_3O_4-CNCC

Fig S1 shows the zeta potentials of different materials. The zeta potentials of NCC and CNCC were measured as –20.46 mV and –30.05 mV, which were ascribed to the high density of the carboxyl groups on the CNCC surface. Therefore hydrophilic CNCC has good dispersiveness and stability. The zeta potential of Fe_3O_4-CNCC was –34.05 mV, which made it easily to be doped in the polymerizing EDOT to neutralize the positive charges on the backbone of PEDOT.

The XRD patterns of CNCC and Fe_3O_4-CNCC composite are shown in Fig S2. The diffraction peaks at 2θ = 16.5°, 22.5° and 34.5° (labeled by the star) correspond to (110), (200) and (004) planes of CNCC respectively.[39] In the case of CNCC-Fe_3O_4 composite, the emerging diffraction peaks were from the (022), (400), (333) and (044) crystallographic planes of cubic structure of Fe_3O_4,[25] indicating that Fe_3O_4 has been successfully modified on CNCC.

The TEM images of the CNCC and Fe_3O_4-CNCC are shown in Fig 2. Clearly, the CNCC was rod-like and the average diameter of CNCC was about 10 nm (Fig 2a). When modified on CNCC, Fe_3O_4 nanoparticles formed uniformly on the surface of CNCC (Fig 2b). PEDOT/CNCC (Fig 2c) exhibited a network-like wrinkled surface morphology. Compared to PEDOT/CNCC, the obtained PEDOT/Fe_3O_4-CNCC (Fig 2d) showed different morphology and the diameter of the PEDOT/Fe_3O_4-CNCC was significantly wider than that of the PEDOT/CNCC.

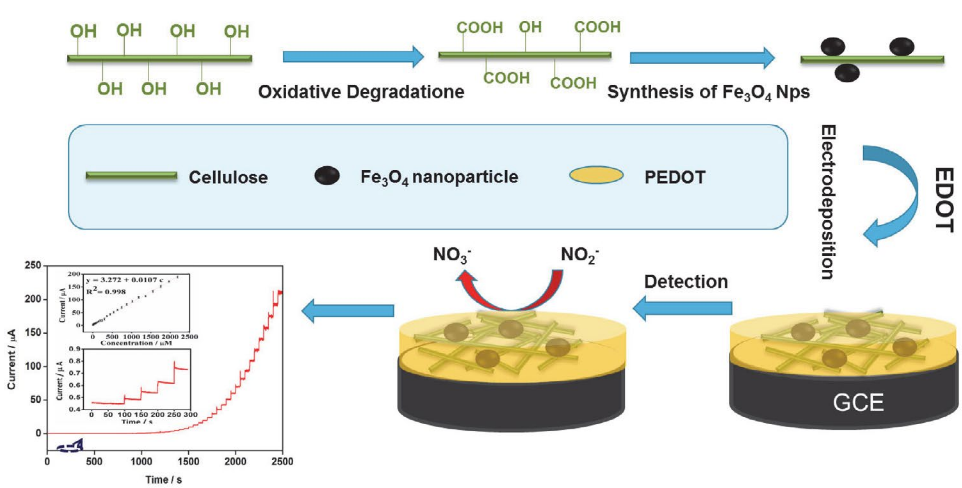

Fig 1. Schematic illustration of the preparation of the PEDOT/Fe_3O_4-CNCC/GCE and the proposed mechanism for the nitrite detection.

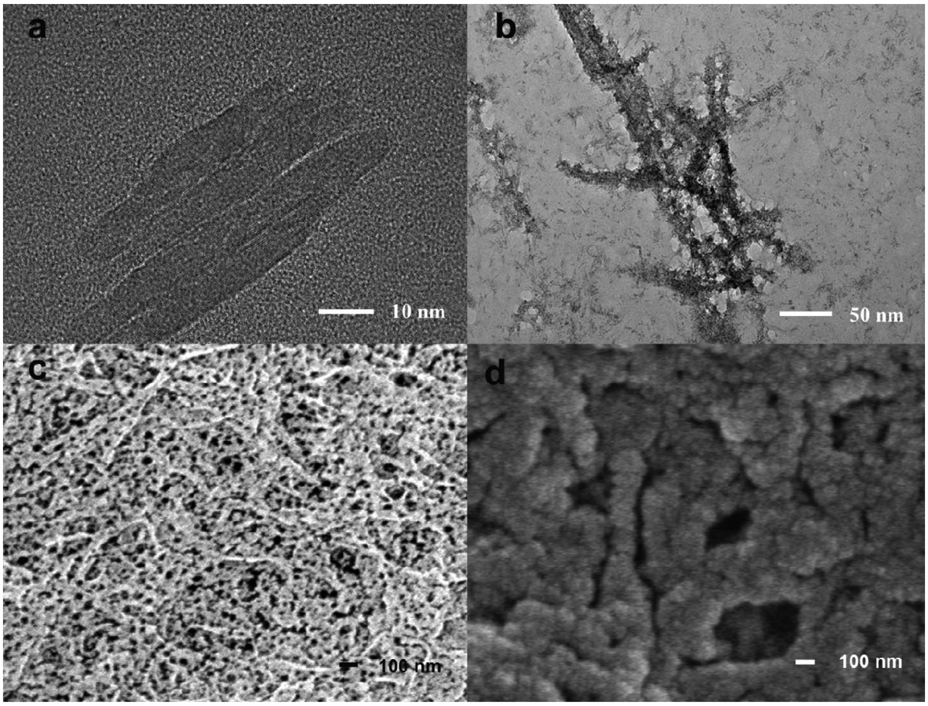

Fig 2. TEM images of CNCC (a), Fe_3O_4-CNCC (b). SEM images of PEDOT/CNCC (c) and PEDOT/Fe_3O_4-CNCC (d).

3. 3. Electrochemical Characterization of PEDOT/Fe_3O_4-CNCC/GCE

CV and EIS were useful tools to research the nature of the modified electrodes and the influence of nanoparticles on electron-transfer kinetics.[40] Fig 3A shows CVs recorded in a 0.1 M KCl aqueous solution containing 5 mM $Fe(CN)_6^{3-/4-}$. The bare GCE (curve a) showed poor electron-transfer kinetics for the $Fe(CN)_6^{3-/4-}$ redox couple with an obvious peak-to-peak separation (ΔE_p). Both the PEDOT/CNCC/GCE (curve b) and PEDOT/Fe_3O_4-CNCC/GCE (curve c) exhibited a reversible redox response. The reversible redox peak currents at PEDOT/Fe_3O_4-CNCC/GCE (curve c) was larger than that at bare GCE and PEDOT/CNCC/GCE, indicating that the introduction of Fe_3O_4 could markedly increase the electron transfer ability of the electrode. The EIS for $Fe(CN)_6^{3-/4-}$ at different electrodes are shown in Fig 3B. The diameter of semicircle could be used to estimate the electron-transfer resistance (Ret) [37]. The Ret value obtained at bare GCE

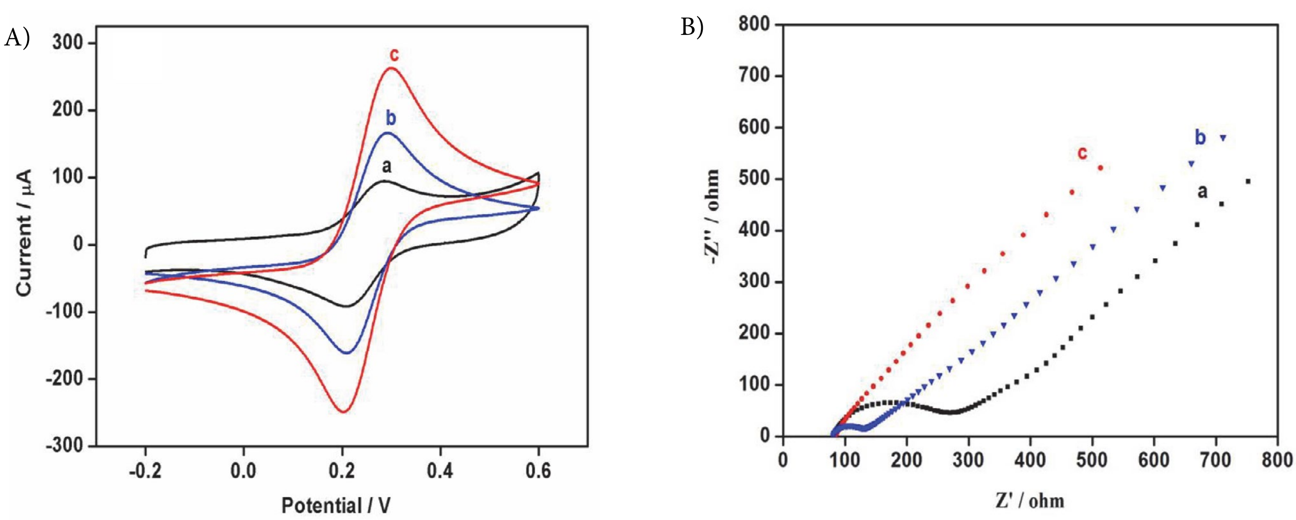

Fig 3. Cyclic voltammograms (A) and electrochemical impedance spectroscopy (B) of 5.0 mM $[Fe(CN)_6]^{3-/4-}$ on bare GCE (a), PEDOT/CNCC/GCE (b), PEDOT/Fe_3O_4-CNCC/GCE (c) in 0.1 M KCl solution. The scan rate is 100 mV s^{-1}.

(curve a, 197.8 Ω) was significantly higher than that of the PEDOT/CNCC/GCE (curve b, 53.54 Ω). The PEDOT/Fe_3O_4-CNCC/GCE (curve c) was linear curve, implying that the Ret was close to zero, which may be ascribed to PEDOT/Fe_3O_4-CNCC composite film being highly conductive and the unique microstructure of the PEDOT/Fe_3O_4-CNCC can increase the effective surface area of the modified electrode. The PEDOT/Fe_3O_4-CNCC/GCE showed much lower electron-transfer resistance than PEDOT/CNCC/GCE and bare GCE, which was quite in agreement with the results obtained from CV.

The real electrochemical surface areas of different electrodes (Fig 4) were characterized by CV in 5 mM $Fe(CN)_6^{3-/4-}$ containing 0.1 M KCl at various scan rates.

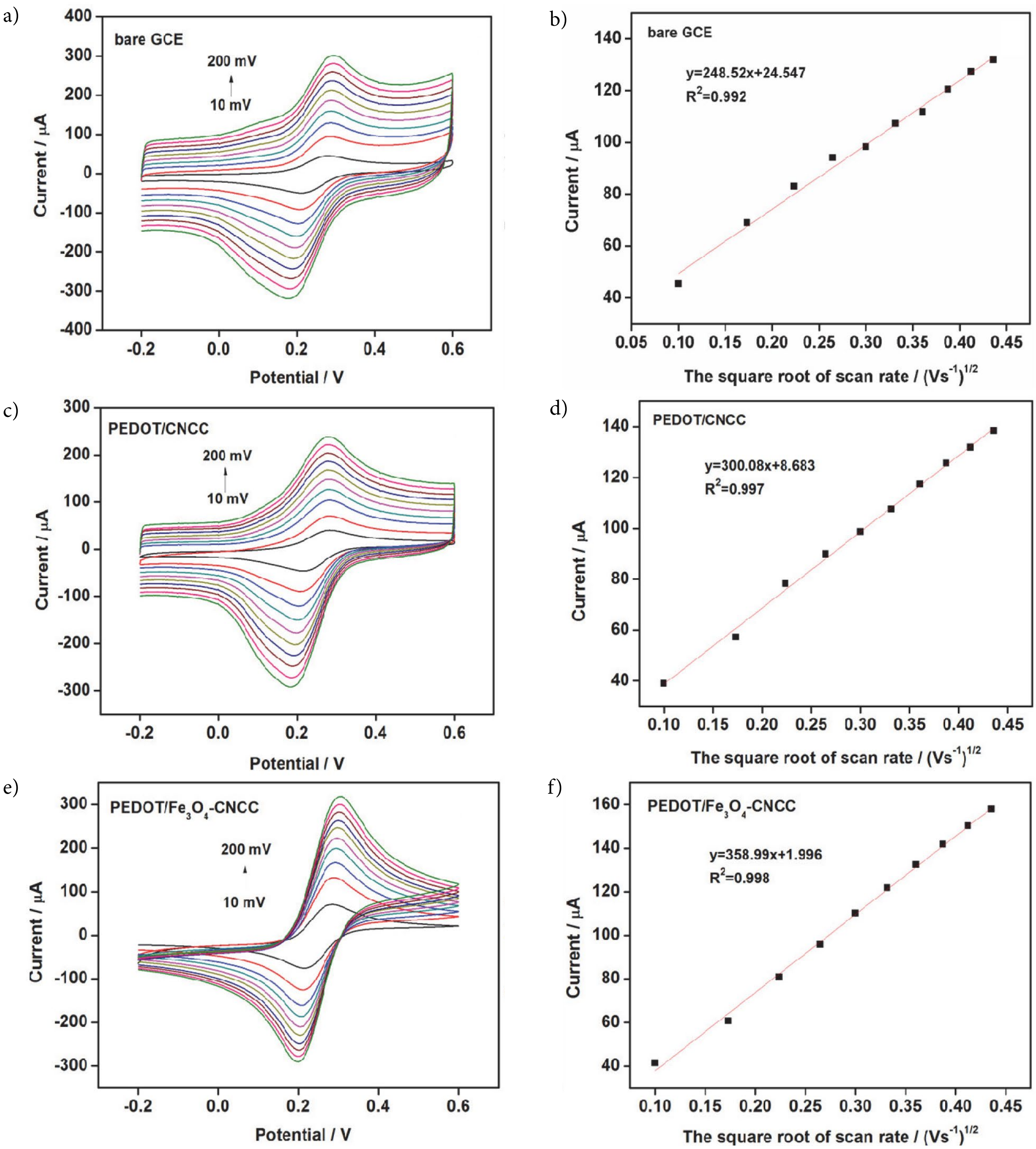

Fig 4. Cyclic voltammograms of 5 mM $Fe(CN)_6^{3-/4-}$at bare GCE (a), PEDOT/CNCC/GCE (c), PEDOT/Fe_3O_4-CNCC/GCE (e) with different scan rate, and (b), (d), (f) the corresponding plots of current at a, c, e versus the square root of the scan rate, respectively.

According to the Randles–Sevcik equation [24], $i_p = (2.69 \times 10^5)\, n^{3/2} A C D^{1/2/} n^{1/2}$, the real electrochemical surface areas of the bare GCE, PEDOT/CNCC/GCE, PEDOT/Fe_3O_4-CNCC/GCE were calculated to be 0.0145, 0.0175, and 0.0209 cm^{-2}, respectively. These results further revealed that the introduction of CNCC and Fe_3O_4 nanoparticles could enlarge the electrochemical active electrode surface.

3. 4. Electrochemical Detection of Nitrite at the PEDOT/Fe_3O_4-CNCC/GCE

The electrochemical response of the different electrodes toward nitrite was examined by CV, as shown in Fig 5. The voltammetric peaks observed at 0.7–1.05 V were ascribed to the oxidation of NO_2^- to NO_3^-. The bare GCE showed no obvious anodic peak after the addition of nitrite (curve a). The oxidation currents and peak potentials of nitrite on the PEDOT/CNCC/GCE (curve b) and PEDOT/Fe_3O_4-CNCC/GCE (curve c) were measured to be 130 μA, 237 μA and 0.88 V, 0.76 V, respectively. More negative oxidation peak potential (~ 0.1 V) confirmed that Fe_3O_4 nanoparticles could notably increase the catalytic activity of the PEDOT/Fe_3O_4-CNCC/GCE.

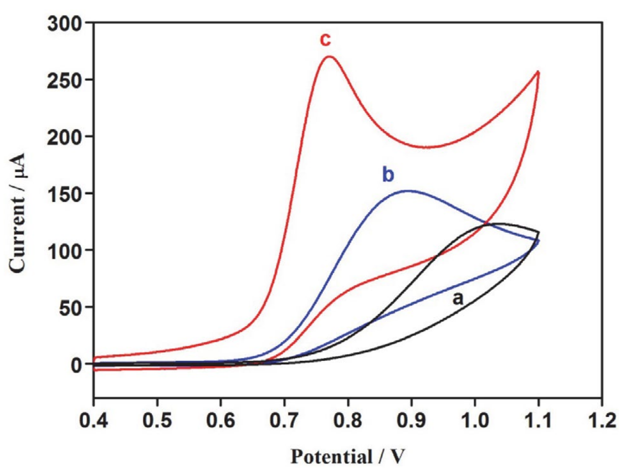

Fig 5. CV curves of different electrodes in PBS (0.2 M, pH 7.4) in the presence of 5.0 mM nitrite at 100 mV s^{-1}: bare GCE (a), PEDOT/CNCC/GCE (b), PEDOT/Fe_3O_4-CNCC/GCE (c).

As shown in S3, DPV detection gave similar results. 5 mM nitrite showed a peak current (I_p) of 38.96 mA with the peak potential of 1.05 V at the bare GCE (a). The I_p of 5 mM nitrite was 100.42 μA at the PEDOT/CNCC/GCE with the peak potential of 0.87 V (b), and 142.2 μA at the PEDOT/Fe_3O_4-CNCC/GCE with the peak potential of 0.80 V (c). Significantly improved peak current and more negative peak potential were obtained for nitrite oxidation at the PEDOT/Fe_3O_4-CNCC/GCE.

The effect of scan rate on the anodic current from nitrite oxidation on the PEDOT/Fe_3O_4-CNCC/GCE was also investigated. As shown in Fig S4A, the oxidation current increased with the increasing of the scan rate and a liner relationship can be obtained between the peak current versus square root of scan rate in the range from 0.05 to 0.19 V/s ($R^2 = 0.997$). The diffusion-controlled irreversible electrochemical process of nitrite oxidation on the PEDOT/Fe_3O_4-CNCC/GCE was determined. Fig S4B also confirmed that sodium nitrite did not adsorb to the electrode surface and therefore did not affect the subsequent experimental determination.

3. 5. Amperometric Response to Nitrite Detection

For better nitrite detection, the effect of deposition time was investigated. As exhibited in Fig 6, when the deposition time reached 180 s, the oxidation peak current of nitrite reached the maximum. With a shorter deposition time, the deposited PEDOT/Fe_3O_4-CNCC was not sufficient, and with a longer deposition time, the thicker PEDOT/Fe_3O_4-CNCC composite will peel off during the reaction. Therefore, 180 s was selected as the optimal deposition time.

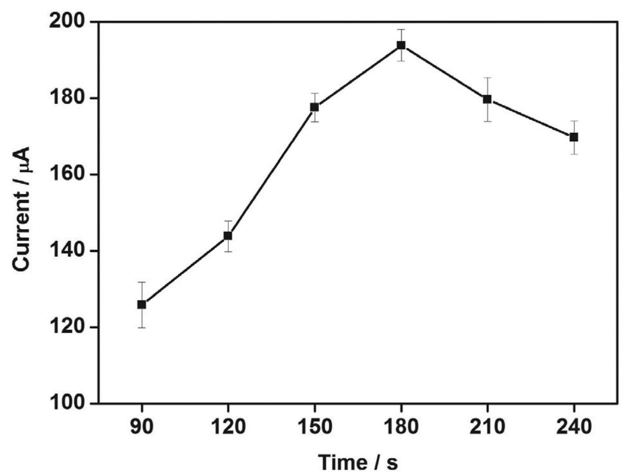

Fig 6. Effects of deposition time on the oxidation peak current of 5.0 mM nitrite at the prepared PEDOT/Fe_3O_4-CNCC/GCE.

The impact of pH on the electro-oxidation behavior of nitrite was analyzed in the pH range from 4.0–8.0 in 0.2 M PBS by DPV technique (Fig 7). The maximum peak current was obtained at pH 7 and then decreased slowly. We chose pH 7.4 for further studies because it was closely related to our physiological pH ranges.

The detection of nitrite with different concentrations at PEDOT/Fe_3O_4-CNCC/GCE was performed under the optimized deposition time. A well-defined anodic peak was observed at about 0.8 V (vs SCE), and the peak current increased with the increase of nitrite concentration (Fig 8). Moreover, the peak current (Ip) has good linear relationship with the concentration (c) of nitrite in a wide range of

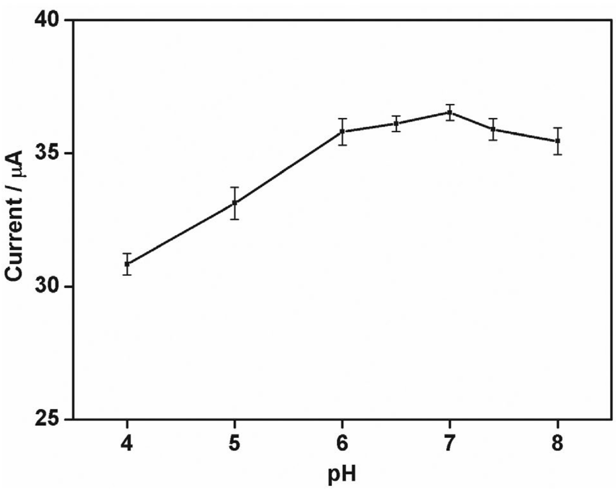

Fig 7. The influence of pH on the oxidation peak current (DPV) of 0.5 mM nitrite at the prepared PEDOT/Fe_3O_4-CNCC/GCE.

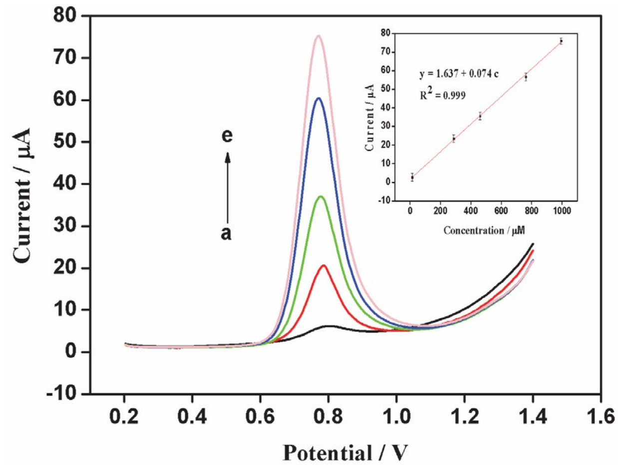

Fig 8. DPVs of nitrite with different concentrations on PEDOT/Fe_3O_4-CNCC/GCE in PBS (0.2 M, pH 7.4) at a scan rate of 100 mV s^{-1}. The inset is the linear relationship between peak currents and concentrations of nitrite.

15 µM to 993 µM. The linear regression equation was determined to be I_p/µA = 0.074 c + 1.637 with a coefficient of R^2 = 0.999, and the limit of detection (LOD) was 15 µM.

In addition, amperometric (i-t) technique was also employed to detect nitrite. From Fig 9, the amperometric current response of the oxidation of nitrite on PEDOT/Fe_3O_4-CNCC/GCE at an applied potential of 0.8 V and the rotation speed of 1200 rpm with successive addition of varying concentrations of nitrite in 0.2 M PBS solution (pH 7.4). The sensor responded quickly to the change of nitrite concentration and achieved a steady state current within 2 s after the injection of nitrite. The linear range for the nitrite electrocatalysis was 0.5–2500 µM with linear regression equation of I_p/µA = 0.079 c + 0.495 (0.50–270.8 µM, R^2 = 0.999) and I_p/µA = 0.074 c + 2.83 (270.8–2500 µM, R^2 = 0.996) The LOD was calculated to be 0.1 µM. We achieved to develop a nitrite sensor with low LOD and wide liner range that is superior to previously reported sensors, as listed in Table 1.

3. 6. Selectivity, Stability, Repeatability, and Reproducibility

The selectivity of a sensor is a crucial factor for its practical application. Some possible interfering substances in electrochemical detection of nitrite, such as ascorbic acid (AA), dopamine (DA), uric acid (UA), sodium citrate and sodium benzoate were added to nitrite solution (Fig 10). Clearly, a large oxidation peak current was obtained in

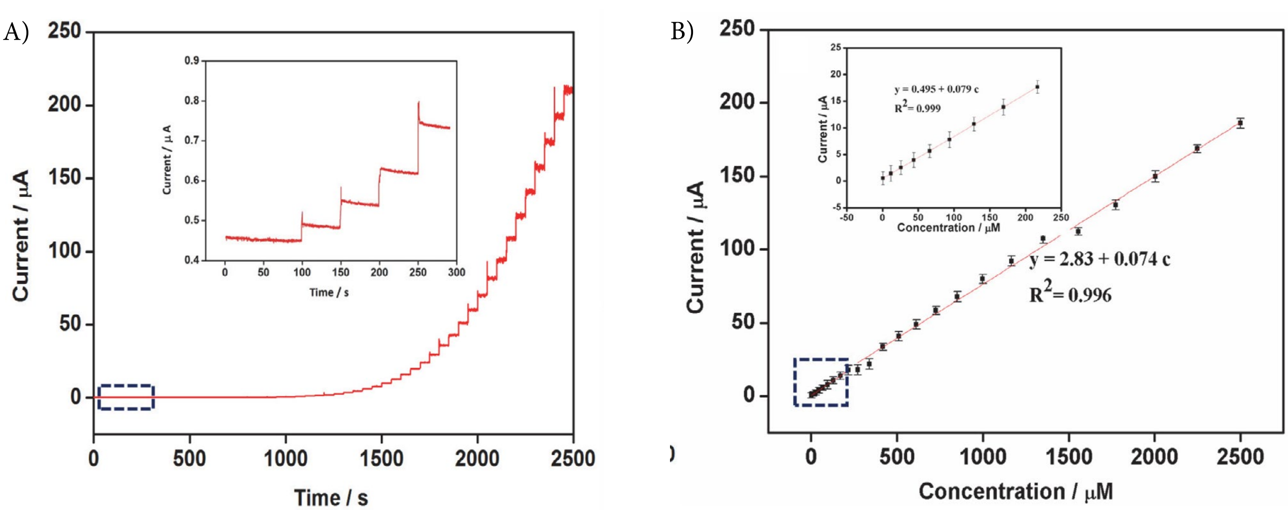

Fig 9. (A) Amperometric responses of the PEDOT/Fe_3O_4-CNCC/GCE in stirring PBS (0.2 M, pH 7.4) at an applied potential of 0.8 V to various concentrations of nitrite from 0.5 mM to 2500 mM. Inset shows the magnified amperometric response to the low nitrite concentration (0.5–5 µM). (B) The corresponding calibration plot for the PEDOT/Fe_3O_4-CNCC/GCE (the nitrite concentrations were 0.50, 11.7, 25.6, 43.7, 65.9, 93.6, 128.0, 216.7, 270.8, 337.7, 417.2, 508.9, 612.1, 726.4, 851.2, 997.9, 1165.2, 1351.2, 1554.2, 1772.4, 2003.9, 2246.9 and 2500.0 µM in sequence). Inset shows the corresponding calibration plot for the low nitrite concentration (0.50–270.8 µM).

Table 1. Comparison of the performances of different electrochemical sensors for the determination of nitrite.

Analysis methods	Material used	Analytical Range [μM]	LOD [mM]	Reference
Amperometric	CeOrGo	0.7–385	0.18	41
Amperometric	PANI-MoS_2	4–4834	1.5	42
DPV	Au-RGO/PDDA	0.05–8.5	0.04	43
DPV	*N*-aceytl-*L*-methionine	1–500	0.75	44
Squre-wavevoltammetry	Cu/MWCNT/RGO	0.1–75	0.03	45
Squre-wavevoltammetry	AgPs-IL	50–1000	3	46
Cyclic voltammetry	CNT-PPy-Pt	0.5–2000	0.5	47
Amperometric	PEDOT/AuNPs	3–300	0.1	48
Amperometric	poly(1,3-DAB) film	10–1000	2	49
Amperometric	cellulose acetate membrane	1–100	0.5	50
Amperometric	PEDOT/Fe_3O_4-CNCC	0.5–2500	0.1	This work

PBS (0.2 M, pH 7.4) containing 0.1 mM nitrite (Fig 10a). After 0.5 mM AA, 0.5 mM DA, 1 mM UA, 1 mM sodium citrate and 1 mM sodium benzoate were added into 0.1 mM nitrite solution, the nitrite oxidation peak current declined by 4% but oxidation peak potential was not changed (Fig 10b). These electroactive species and food additives have no obvious interference on the determination of nitrite. The developed sensor can easily distinguish DA, AA, UA, and nitrite. The results suggested that the PEDOT/Fe_3O_4-CNCC exhibited high selectivity for nitrite detection.

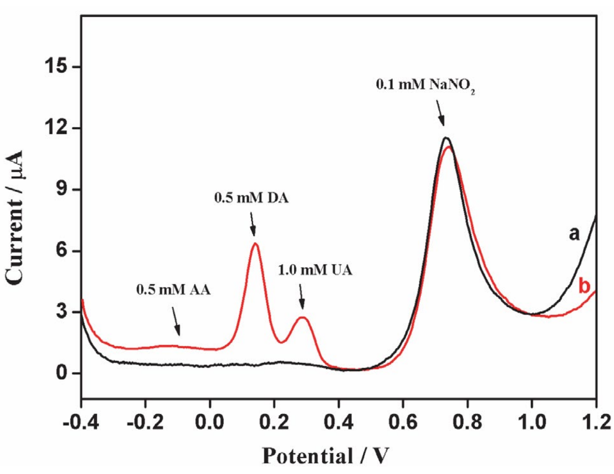

Fig 10. DPVs of the PEDOT/Fe_3O_4-CNCC/GCE in the absence (a) and presence (b) of 0.5 mM AA, 0.5 mM DA, 1.0 mM UA, 1 mM sodium citrate and 1 mM sodium benzoate in PBS (0.2 M, pH 7.4) containing 0.1 mM nitrite.

The selectivity of proposed sensor was also evaluated by amperometric method at the potential of 0.8 V. A 0.1 mM amount of nitrite, 0.5 mM AA, 0.5 mM DA, 1.0 mM UA, 1.0 mM sodium citrate, 1.0 mM sodium benzoate, and a second injection of 0.1 mM nitrite were added into PBS (pH 7.4) to investigate the selectivity of the PEDOT/Fe_3O_4-CNCC/GCE. Figure S5 displays that the addition of AA, DA, and UA exhibited measurable current responses. DPV method should be used when nitrite coexists with AA, DA, and (or) UA in biological samples to avoid the interferences.

The stability of PEDOT/Fe_3O_4-CNCC/GCE was investigated by amperometric (i-t) technique in 0.2 M PBS with the presence of 200 μM nitrite. The current response of nitrite oxidation was recorded over a long operational period of 2500 s and retained about 96.7% of its original current. Furthermore, the PEDOT/Fe_3O_4-CNCC/GCE was fabricated and the nitrite oxidation response monitored for 2 weeks. The prepared sensor achieved 95.3% of efficiency towards the detection of nitrite, revealing the excellent long-term stability. The repeatability was observed for 10 consecutive measurements with one modified electrode in the presence of 200 μM nitrite with relative standard deviation (RSD) of 4.6%, suggesting an acceptable repeatability of the PEDOT/Fe_3O_4-CNCC modified electrode. In addition, three independent PEDOT/Fe_3O_4-CNCC modified electrodes were chosen for the determination of nitrite with an RSD of 3.7% that displayed a good reproducibility.

3. 7. Determination of Nitrite in Pickles

To demonstrate the practical feasibility of such an electrochemical sensor, the PEDOT/Fe_3O_4-CNCC/GCE was used to detect nitrite in pickles. The pickle samples were purchased from the local market in Qingdao, Shandong, and were pretreated as follows. The samples were ground adequately in a juicer, a portion of 10 g of puree was mixed with 50 mL of water, followed by sonication for 30 min in a beaker. Then the resulting mixture was centrifuged for 10 min at 4000 rpm. Finally, the supernatant was diluted to 100 mL using 0.2 PBS (pH 7.4). The recovery of nitrite was calculated using the standard addition method. The standard HPLC method was employed for the comparison. Table 2 lists the results obtained by these two

Table 2. Results of the determination of nitrite in pickles (n = 4).

Samples	The proposed electrochemical method					HPLC method	
	Detected [mg kg^{-1}]	Added [μM]	Found [μM]	Recovery [%]	RSD [%]	Detected [mg kg^{-1}]	Relative error[%]
1	3.48	10	9.65	96.5	3.01	3.62	3.87
2	3.57	20	19.54	97.7	2.86	3.47	–2.88
3	3.73	30	30.60	102	2.71	3.92	4.85
4	4.21	40	39.76	99.4	2.94	4.32	2.55

methods. The recoveries from 96.5% to 102% suggest that results from the proposed method are comparable with those from HPLC. Noticeably, without the use of extraction columns which are required for HPLC, the simple and rapid pretreatment of the proposed method is suitable for on-site detection. These results imply the good accuracy, reliability, and feasibility of PEDOT/Fe_3O_4-CNCC/GCE for the detection of nitrite in pickle samples.

4. Conclusions

A simple electrochemical sensor was developed based on PEDOT/Fe_3O_4-CNCC composite and used to determine nitrite. It is confirmed that rod-like CNCC works as a substrate and the Fe_3O_4 magnetite nanoparticles grow on the surface of CNCC. The prepared Fe_3O_4-CNCC nanocomposite can be doped into PEDOT to enhance its electrical conductivity. As a key element of the nitrite sensor, the PEDOT/Fe_3O_4-CNCC nanocomposite combines the advantages of CNCC and Fe_3O_4, as well as PEDOT, and can enhance the measurement of nitrite. The PEDOT/Fe_3O_4-CNCC/GCE has been applied to determine nitrite with high selectivity, low detection limit (0.1 mM), large linear range (0.5–2450 μM) and outstanding stability and reproducibility. More importantly, the electrochemical sensor based on PEDOT/Fe_3O_4-CNCC has shown great potential application for nitrite detection in food safety analysis.

5. Acknowledgements

This research was supported by the National Natural Science Foundation of China (21675093), the Natural Science Foundation of Shandong Province of China (JQ201406, ZR2016BM05), and the Science and Technology Project of Shandong Province (J15LC14).

6. References

1. S. J. Eichhorn, A. Dufresne, M. Aranguren, N. E. Marcovich, J. R. Capadona, S. J. Rowan, C. Weder, W. Thielemans, M. Roman, S. Renneckar, W. Gindl, S. Veigel, J. Keckes, H. Yano, K. Abe, M. Nogi, A. N. Nakagaito, A. Mangalam, J. Simonsen, A. S. Benight, A. Bismarck, L. A. Berglund, T. Peijs, *J. Mater. Sci.* **2010**, *45*, 1–33. **DOI:**10.1007/s10853-009-3874-0
2. Y. Habibi, L. A. Lucia, O. J. Rojas, *Chem. Rev.* **2010**, *110*, 3479–3500. **DOI:**10.1021/cr900339w
3. R. J. Moon, A. Martini, J. Nairn, J. Simonsen, J. Youngblood, *Chem. Soc. Rev.* **2011**, *40*, 3941–3994. **DOI:**10.1039/C0CS00108B
4. N. Lin, J. Huang, A. Dufresne, *Nanoscale*. **2012**, *4*, 3274–3294. **DOI:**10.1039/C2NR30260H
5. C. Salas, T. Nypelö, C. Rodriguez-Abreu, C. Carrillo, O. J. Rojas, *Curr. Opin. Colloid Interface Sci.* **2014**, *19*, 383–396. **DOI:**10.1016/j.cocis.2014.10.003
6. B. L. Peng, N. Dhar, H. L. Liu, K. C. Tam, *Can. J. Chem. Eng.* **2011**, *89*, 1191–1206. **DOI:**10.1002/cjce.20554
7. J. K. Jackson, K. Letchford, B. Z. Wasserman, L. Ye, W. Y. Hamad, H. M. Burt, *Int. J. Nanomed.* **2011**, *6*, 321. **DOI:**10.2147%2FIJN.S16749
8. A. C. W. Leung, E. Lam, J. Chong, S. Hrapovic, J. H. T. Luong, *J. Nanopart. Res.* **2013**, *15*, 1636. **DOI:**10.1007/s11051-013-1636-z
9. M. Kaushik, A. Moores, *Green Chem.* **2016**, *18*, 622–637. **DOI:**10.1039/C5GC02500A
10. A. Kafy, A. Akther, L. Zhai, H. C. Kim, J. Kim, *Synth. Met.* **2017**, *223*, 94–100. **DOI:**10.1016/j.synthmet.2016.12.010
11. R. Liu, L. Ma, S. Huang, J. Mei, J. Xu, G. Yuan, *New J. Chem.* **2017**, *41*, 857–864. **DOI:**10.1039/C6NJ03107B
12. Y. Liu, Z. Shi, Z. Gao, W. An, Z. Cao, J. Liu, *ACS Appl. Mater. Interfaces.* **2016**, *8*, 28283–28290. **DOI:**10.1021/acsami.5b11558
13. X. Wei, T. Huang, J. Yang, N. Zhang, Y. Wang, Z. Zhou, *J. Hazard. Mater.* **2017**, *335*, 28–38. **DOI:**10.1016/j.jhazmat.2017.04.030
14. A. Jasim, M. W. Ullah, Z. Shi, X. Lin, G. Yang, *Carbohydr. Polym.* **2017**, *163*, 62–69. **DOI:**10.1016/j.carbpol.2017.01.056
15. M. G. Bekaroğlu, Y. İşçi, S. İşçi, *Mater. Sci. Eng.* **2017**, *78*, 847–853. **DOI:**10.1016/j.msec.2017.04.030
16. M. Han, X. Jin, H. Yang, X. Liu, Y. Liu, S. Ji, *Carbohydr. Polym.* **2017**, *172*, 223–229. **DOI:**10.1016/j.carbpol.2017.05.049
17. A. M. El-Nahas, T. A. Salaheldin, T. Zaki, H. H. EI-Maghrabi, A. M. Marie, S. M. Morsy, N. K. Allam, *Chem. Eng. J.* **2017**, *322*, 167–180. **DOI:**10.1016/j.cej.2017.04.031
18. E. Lam, A. C. W. Leung, Y. Liu, E. Majid, S. Hrapovic, K. B.

Male, J. H. T. Luong, *ACS Sustainable Chem. Eng.* **2012**, *1*, 278–283. **DOI:**10.1021/sc3001367
19. C. T. Yavuz, J. T. Mayo, W. W. Yu, A. Prakash, J. C. Falkner, S. Yean, L. Cong, H. J. Shipley, A. Kan, M. Tomson, D. Natelson, V. L. Colvin, *Science* **2006**.
20. X. Z. Yao, Z. Guo, Q. H. Yuan, Z. G. Liu, J. H. Liu, X. J. Huang, *ACS Appl. Mater. Interfaces* **2014**, *6*, 12203–12213. **DOI:**10.1021/am501617a
21. J. Zhu, S. A. Baig, T. Sheng, Z. Lou, Z. Wang, X. Xu, *J. Hazard. Mater.* **2015**, *286*, 220–228. **DOI:**10.1016/j.jhazmat.2015.01.004
22. J. Giménez, M. Martínez, J. de Pablo, M. Rovira, L. Duro, *J. Hazard. Mater.* **2007**, *141*, 575–580. **DOI:**10.1016/j.jhazmat.2006.07.020
23. W. Yang, A. T. Kan, W. Chen, M. B. Tomson, *Water Res.* **2010**, *44*, 5693–5701. **DOI:**10.1016/j.watres.2010.06.023
24. L. Wang, Y. Zhang, C. Cheng, X. Liu, H. Jiang, X. Wang, *ACS Appl. Mater. Interfaces.* **2015**, *7*, 18441–18449. **DOI:**10.1021/acsami.5b04553
25. J. Wei, S. S. Li, Z. Guo, X. Chen, J. H. Liu, X. J. Huang, *Anal. Chem.* **2015**, *88*, 1154–1161. **DOI:**10.1021/acs.analchem.5b02947
26. G. Xu, S. Liang, J. Fan, G. Sheng, X. Luo, *Microchim. Acta.* **2016**, *183*, 2031–2037. **DOI:**10.1007/s00604-016-1842-3
27. W. Wang, G. Xu, X. T. Cui, G. Sheng, X. Luo, *Biosens. Bioelectron.* **2014**, *58*, 153–156. **DOI:**10.1016/j.bios.2014.02.055
28. M. Cui, Z. Song, Y. Wu, B. Guo, X. Fan, X. Luo, *Biosens. Bioelectron.* **2016**, *79*, 736–741. **DOI:**10.1016/j.bios.2016.01.012
29. G. Xu, B. Li, X. Luo, *Sens. Actuators, B.* **2013**, *176*, 69–74. **DOI:**10.1016/j.snb.2012.09.001
30. Z. T. Zhu, J. T. Mabeck, C. Zhu, N. C. Cady, C. A. Batt, G. G. Malliaras, *Chem. Commun.* **2004**, *13*, 1556–1557. **DOI:**10.1039/B403327M
31. L. Jiang, R. Wang, X. Li, L. Jiang, G. Lu, *Electrochem. Commun.* **2005**, *7*, 597–601. **DOI:**10.1016/j.elecom.2005.04.009
32. R. Ojani, J. B. Raoof, E. Zarei, *Electrochim. Acta* **2006**, *52*, 753–759. **DOI:**10.1016/j.elecom.2005.04.009
33. R. Yue, Q. Lu, Y. Zhou, *Biosens. Bioelectron.* **2011**, *6*, 4436–4441. **DOI:**10.1016/j.bios.2011.04.059
34. H. Zhang, L. Zhang, C. Lu, L. Zhao, Z. Zheng, *Spectrochimica Acta, Part A* **2012**, *85*, 217–222. **DOI:**10.1016/j.saa.2011.09.063
35. K. J. Huang, W. Z. Xie, H. S. Zhang, H. Wang, *Microchim. Act.* **2008**, *161*, 201–207. **DOI:**10.1007/s00604-007-0784-1
36. Y. Wang, J. Qu, R. Wu, R. Wu, P. Lei, *Water Res.* **2006**, *40*, 1224–1232. **DOI:**10.1016/j.watres.2006.01.017
37. M. A. Kamyabi, F. Aghajanloo, *J. Electroanal. Chem.* **2008**, *614*, 157–165. **DOI:**10.1016/j.jelechem.2007.11.026
38. Ministry of Health of the People's Republic of China, National Food Safety Standard, Determination of Nitrite and Nitrate in Foods, GB 5009. 33–2016, 2016.
39. H. Wang, F. Wen, Y. Chen, T. Sun, Y. Meng, Y. Zhang, *Biosens. Bioelectron.* **2016**, *85*, 692–697. **DOI:**10.1016/j.bios.2016.05.078
40. D. Wang, J. Wang, Z. Liu, X. Yang, X. Hu, J. Deng, N. Yang, Q. Wan, Q. Yuan, *ACS Appl. Mater. Interfaces.* **2015**, *8*, 28265–28273. **DOI:**10.1021/acsami.5b08294
41. D. M. Stanković, E. Mehmeti, J. Zavašnik, K. Kalcher, *Sens. Actuators, B* **2016**, *236*, 311–317. **DOI:**10.1016/j.snb.2016.06.018
42. Y. Zhang, P. Chen, F. Wen, C. Huang, H. Wang, *Ionics* **2016**, *22*, 1095–1102. **DOI:**10.1007/s11581-015-1634-5
43. S. Jiao, J. Jin, L, Wang, *Sens. Actuators, B* **2015**, *208*, 36–42. **DOI:**10.1016/j.snb.2014.11.020
44. A, Kannan, A, Sivanesan, G, Kalaivani, *RSC Adv.* **2016**, *6*, 96898–96907. **DOI:**10.1039/C6RA18440E
45. J. Dai, D. Deng, Y. Yuan, J. Zhang, F. Deng, S. He, *Microchim. Acta* **2016**, *183*, 1553–1561. **DOI:**10.1007/s00604-016-1773-z
46. E. Menart, V. Jovanovski, S. B. Hočevar, *Electrochem. Commun.* **2015**, *52*, 45–48. **DOI:**10.1016/j.elecom.2015.01.017
47. S. Rajesh, A. K. Kanugula, K. Bhargava, G. Llavazhagan, S. Kotmraju, C. Karunakaran, *Biosens. Bioelectron.* **2010**, *26*, 689–695. **DOI:**10.1016/j.bios.2010.06.063
48. O. Zhang, Y. Wen, J. Xu, L. Lu, X. Duan, H. Yu, *Synth. Met.* **2013**, *164*, 47–51. **DOI:**10.1016/j.synthmet.2012.11.013
49. V. Biagiotti, F Valentini, E. Tamburri, M. L. Terranova, D. Moscone, G. Palleschi, *Sens. Actuators, B* **2007**, *122,* 236–242. **DOI:**10.1016/j.snb.2006.05.024
50. M. Badea, A. Amine, G. Palleschi, D. Moscone, G. Volpe, A. Curulli, *J. Electroanal. Chem.* **2001**, *509*, 66–72. **DOI:**10.1016/S0022-0728(01)00358-8

Povzetek

Karboksilirano nanokristalinično celulozo (CNCC) smo pripravili z oksidativnim razkrojem mikrokristalinične celuloze (MCC) z amonijevim peroksidisulfatom in jo modificirali z Fe_3O_4 nanodelci ter pridobili Fe_3O_4-CNCC nanokompozitni material s preprostim postopkom z refluksom. Z Fe_3O_4-CNCC nanokompozitom dopirani poli(3,4-etilendioksitiofen) (PEDOT) smo uspešno nanesli na elektrodo iz steklastega ogljika (GCE) z elektrokemično depozicijo. GCE modificirana z PEDOT/Fe_3O_4-CNCC je imela večjo elektrokemično-aktivno površino in smo jo uporabili za določitev nitrita z visoko selektivnostjo, občutljivostjo in izjemno obnovljivostjo. Ob uporabi amperometrične tokovno-časovne (i-t) krivulje je predlagani senzor imel širše linearno območje (0,5–2500 μM) in nižjo mejo zaznave (0,1 μM) za nitrit v primerjavi z metodo diferencialne pulzne voltametrije (DPV). Predlagana analizna metoda je pokazala dobro selektivnost pri praktičnem določanju nitrita v vloženi zelenjavi.